A HIGH PERFORMANCE SPOT SIZE MONITOR*

M. C. Ross, R. Alley, D. Arnett, E. Bong, W. Colocho, J. Frisch, S. Horton-Smith, W. Inman, K. Jobe, T. Kotseroglou, D. McCormick, J. Nelson, M. Scheeff, S. Wagner, M. Woods

Stanford Linear Accelerator Center, Stanford, California, 94309.

Abstract

Beam size estimates made using beam-beam deflections are used for optimization of the Stanford Linear Collider (SLC) electron-positron beam sizes. Beam size and intensity goals for 1996 were 2.1 x 0.6 μm (x,y) at 4.0x10 ^{10} particles per pulse. Conventional profile monitors, such as scanning wires, fail at charge densities well below this. Since the beam-beam deflection does not provide single beam information, another method is needed for Interaction Region (IP) beam size optimization. The laser based profile monitor uses a finely focused 349 nm. wavelength , frequency-tripled YLF laser pulse that traverses the particle beam path about 29 cm away from the e+/e- IP. Compton scattered photons and energy degraded e+/e- are detected as the beam is steered across the laser pulse. The laser pulse has a transverse size, (σ_0,), of 380 nm and a Rayleigh range of about 5 μm. This is adequate for present or planned SLC beams. Design and results are presented.

Introduction

The Stanford Linear Collider (SLC) is the first of a new generation of colliding beam machines that rely on micron sized beams colliding at a relatively low repetition rate [1]. The ultimate performance of the collider is limited by the control of emittance dilution effects that increase the transverse beam size ($\sigma_{x,y}$) at the interaction point (IP), where the two beams meet each other. A useful estimate of $\sigma_{x,y}$ is obtained from the deflection seen when sweeping one beam across the other [2]. The two principle drawbacks of the deflection technique are its sensitivity to shifts in beam centroid and a lack of indication of which beam is changing.

The latter has the most significant impact on emittance dilution and optics related optimization. A single beam (e+ or e-) diagnostic that can operate over the full range of SLC beam intensities from 0.3 x 10^{10} to 4 x 10^{10} particles per bunch is needed. Unfortunately, wire scanners cannot be used for beam sizes smaller than 1.4 μm or for intensities greater than 0.6 x 10^{10}. A wire scanner equipped with 4 μm diameter carbon wire is used to measure $\sigma_{x,y}$ for beams safely away from these thresholds. If either threshold is exceeded, the energy deposited in the wire from a single pulse severs it. The wire scanner is installed deep inside the solenoidal SLC Large Detector (SLD) system and is virtually inaccessible, so routine replacement of the carbon wires is not practical.

The SLC IP laser based beam profile monitor will be used to measure $\sigma_{x,y}$ of individual beams inside the SLD over the full range of operating intensities with about 10% accuracy. Some key features of the device are similar to the laser based beam size monitor developed for the FFTB at SLAC [3][4]. A finely focused laser pulse is brought into a 90˚ crossing angle collision with the electron and positron beam and the Compton scattered photons and degraded beam particles are detected. As the e+/e- beams are steered across the laser pulse on a succession of pulses, the amplitude of the scattered radiation is recorded and used to estimate the beam sizes, in a manner similar to that used with SLC wire scanners [5].

Future linear colliders (NLC) will employ beams of higher charge density than those of SLC [6]. In most designs, conventional wire scanner limits will be exceeded for all damped beam regions. Sets of laser based monitors will serve as emittance monitors. Lessons learned from the operation of the device described in this paper will be useful for the development of NLC beam profile monitors.

Principle of Operation

We considered three basic 'optical scattering structures', 1) a diffraction limited, finely focused waist (TEM'00' mode), 2) an interference fringe pattern similar to that used at FFTB and 3) the finely focused waist of a first order transverse mode laser beam (TEM'01' mode).

The minimum transverse size, σ_0, of a diffraction limited laser beam is [7]:

$$\sigma_0 = \frac{\lambda f}{4\pi\sigma_{in}}.$$

where λ is the wavelength of the light, f is the focal length of the lens and σ is the gaussian beam sigma as defined by the photon density. The effective length of the focused section is twice the Rayleigh range (z_R).

$$2z_R = \frac{8\pi\sigma_0^2}{\lambda} \text{ where } \sigma(z_R) = \sqrt{2}\sigma_0.$$

The incoming beam size, σ_{in}, and f combine to give an '*f#*', with the aperture roughly $\pm 3\ \sigma_{in}$ giving $\sigma_0 \sim 1/2\ f\#\ \lambda$. For typical SLC parameters, with the required beam stay clear distance of 25mm and an *f#* of 2, λ must be shorter than 500 nm in order to have $\sigma_0 < \sigma_y$ and $z_R \sim 5\mu$m. This is the option selected.

The second 'optical scattering structure', the interference fringe pattern, is useful for much smaller beam sizes than those expected for SLC and, unless the pattern pitch is controllable, can be used to measure only a small range of beam sizes. Scanning with this system involves measuring the modulation

* Work supported by Department of Energy Contract DE-AC03-76SF00515

depth of the scattered radiation as the beam is moved across the pattern. We could not find room in the confines of SLD for fringe pitch control.

The third option mentioned above, the TEM '01' mode laser beam, with a field null at the center of the spot, may prove useful. It is easy to implement since the mode would be generated at the laser and the modest increase in σ_{in} is accommodated in the transport and IP optics. A double lobed result is generated from a '01' mode scan and the spacing between the lobes can be used a laser beam diagnostic.

As the particle beam is swept over the laser beam with a varying impact parameter y_0, the number of scattered photons, $N_\gamma(y_0)$, is given by:

$$N_\gamma(y_0) = \frac{PN_e\sigma_c}{ch\nu\sqrt{2\pi}\sigma_s} exp(\frac{-y_0^2}{2\sigma_s^2})$$

where P is the power of the laser beam intercepted by the particle beam (σ_z=750μm), ν is the frequency of the laser light, N_e is the number of electrons in the beam, σ_c is the Compton scattering cross section and σ_s is the overlap size ($\sigma_s^2 = \sigma_y^2 + \sigma_0^2$). For peak laser power of 10MW and with σ_y = 1μm and $N_e = 10^{10}$, N_γ is ~5000. A correction, nominally about 12%, is required since the particle beam has an aspect ratio (σ_y/σ_x) ~ 5 and the laser spot does not have a ellipsoidal cross section.

The energy distribution of the scattered photons and degraded beam particles is relatively flat and, for λ=350 nm (3rd harmonic YLF), has a peak gamma radiation energy of 29GeV for SLC. Detectors for monitoring the gamma rays and the degraded e+/e- particles are located along the beamline that extends to the beam dump area [8],[9]. Backgrounds in the degraded particle detectors are typically about 50 particles per beam crossing.

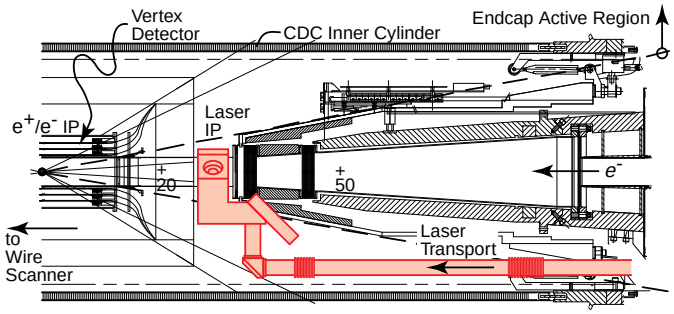

Figure 1. Cutaway elevation view of the inside of the SLD. The new vertex detector [10], surrounding the e+/e- IP with the wire scanner on one side (not shown) and the laser profile monitor on the other, is itself surrounded by the 13 inch inner cylinder of the SLD central tracking drift chamber (CDC). Access is not available beyond a few inches from the end of the cylinder. The laser transport line (shaded) enters from the bottom right of the figure and passes through two bellows before terminating in the IP optics bench. The numbers along the central axis indicate the distance in cm from the e+/e- IP.

Optics

Optics design goals were to achieve the minimum σ_0 with the highest transmitted power and the lowest possible aberrations. The most important mechanical constraints were the minimum beam transport diameter of 25mm, the available beamline length of 52mm and mass and density restrictions. Figure 1 shows an elevation view of the IP layout. Within the cone subtended by active SLD segments, the mass of the optics and related supports must cause minimal scattering of the decay particles the SLD is intending to analyze.

The IP *f*2 optics (figure 2) are catadioptric, with minimal geometric aberrations, in which a diverging meniscus lens is coupled with a spherical reflector [11]. Two such systems are required, for measuring both σ_x and σ_y. For laser pulse lengths longer than about 150ps, the particle beam will also scatter some of the incoming photons before they reflect from the spherical mirror.

The incoming laser beam has σ_{in} of about 2.5mm. As σ_{in} is increased, diffraction scattering from the edges of the input optic produces non-gaussian tails effectively increasing σ_0. For small σ_{in}, the effective *f#* of the IP is increased, resulting in a larger σ_0. At the end of the transport, in the IP 'optics bench' (fig. 3), a compact switch system is used to select which of the two possible paths through the IP the laser will follow. A brewster polarizer is used in conjunction with a linear polarizer at the laser to do the selection. A compact construction was required in order to minimize the mass obscuring the SLD end cap detector segments and in order to fit around SLD internal masking and supports.

An estimate of the deviation from diffraction limit caused by surface figure distortions yielded a per element mirror and lens surface figure tolerance of λ/40.

Laser Induced Optical Component Damage

Since we require reliable operation for several years, about 100 million pulses, and since much of the system is sealed and inaccessible, considerable design effort was concentrated on damage prevention. In order to prevent inadvertent high power density related damage, no lenses or other focusing elements are present in the transport line that carries the light from the laser room to the IP.

The most threatening source of damage is from chemical contaminants. Studies of damage in sealed laser systems (typically infrared lasers) have shown that organic chemical contaminants are a leading cause[12]. Trace contaminants, such as silicone sealers, have been pinpointed as root causes. There is little information available concerning the long term operation of UV lasers where it is possible that the sensitivity to trace organic chemicals will be greater. For this reason, our design transport σ is as large as possible and all IP, IP bench and transport assembly took place in class 100 clean rooms. Non-ultra high vacuum (UHV) volumes are purged with an Ar/O_2 (90/10) mixture as suggested in the report noted above.

Bulk multi-photon damage is another serious concern for long term operation of the UV system with several

transmissive optics. Darkening in fused silica has been seen following long term exposure to high fluence, short wavelength light [13]. We interpolated between results at 248nm and at 550nm and set our tolerance a factor 5 away from the threshold where these effects are first seen.

Mechanical

Three subsystems, the IP and its mirror bench, the 17m transport line and the laser itself comprise the profile monitor. The laser is housed in a external clean room. The transport line passes through the beamline radiation shielding and then along the superconducting quadrupole triplet before entering the SLD vertex area.

The beam enters the IP, (figure 2), from the right or from the bottom, for *y* or *x* scans respectively, and passes through the UHV fused silica window that separates the gas filled optics bench from the beamline vacuum. A seal design was developed that allowed the window surfaces to be ground to λ/40 surface quality after attaching the weld ring. The window is coated with a graded index 'Solgel' anti-reflective [14] coating. Conventional dielectric layer coatings were rejected since their application would be made after the attachment of the weld ring.

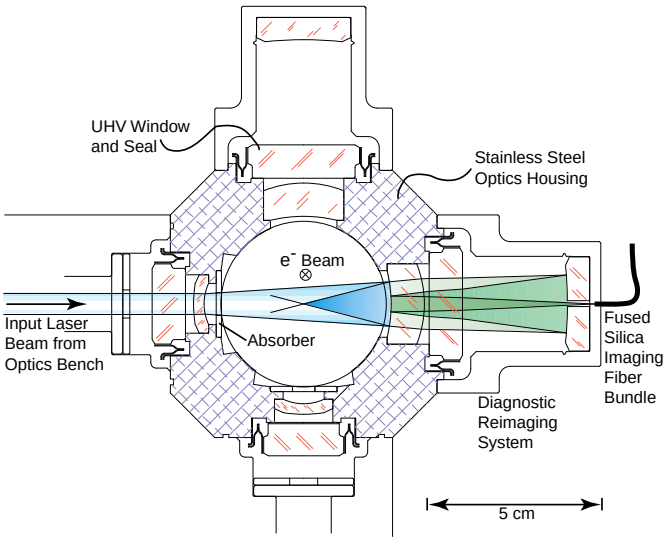

Figure 2.Central cross section of IP Optics. The parallel laser beam (z_R>> 20m) enters at right or from underneath with a σ_{in} of about 2.5mm. The four 8mm thick UHV seal windows with their weld rings are placed on each side of the IP, with the precision optics installed inside the vacuum chamber. 1% of the light is transmitted and re-imaged on the far side of the IP for diagnostic purposes.

After passing through the focal point the spent laser light is absorbed using glass absorbers located both inside and outside the vacuum system. This prevents possible reflection from metal surfaces that might make secondary ghost images or sputter nearby metal surfaces and thereby cause damage to optical components. The spherical reflector coating allows 1% of the incident light to pass through. Its rear surface, together with a second spherical reflector outside of the vacuum chamber, generate an image of the IP spot that is used as a diagnostic.

The IP optics bench directs the light from the transport to the IP using one controllable and 4 fixed mirrors. It terminates the 1 inch diameter laser transport line. The transport line is evacuated for 90% of its length (10^{-6} Torr) and slightly pressurized, along with the optics bench, for the remaining 10%. This section is flexible, to be compliant in seismic events, and removable, to allow servicing SLD luminosity components.

The IP housing has a required vacuum performance of 5 nano-Torr. The catadioptric optics are most sensitive to lens and mirror centering and coplanarity errors which lead to machining tolerances of 5μm.

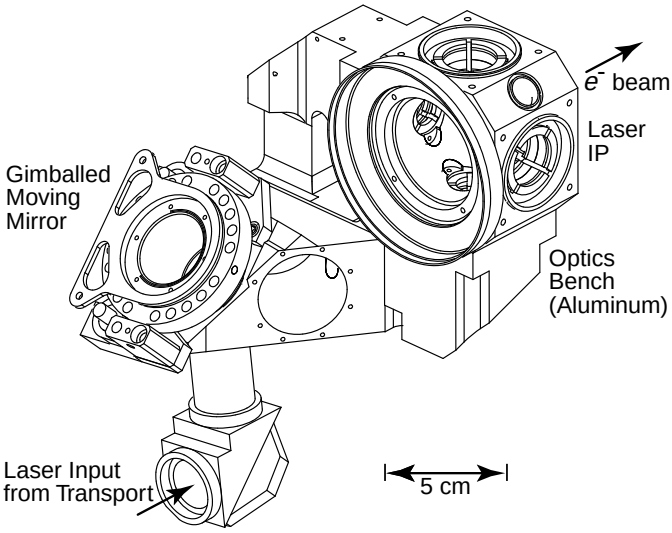

Figure 3. IP Optics Bench Machining. The bench contains 5 mirrors and a Brewster angle polarizer. It has 2.2cm diameter machined internal passages for light transport. The IP is in the top right of the figure, shown without the diagnostic re-imaging optics installed. Eight mirror retaining cap mounting holes are clearly visible in the front of the figure.

A gimbaled moving mirror mount was developed for the transport line that has angular stability of 30μrad and compensated bellows vacuum forces. Fine alignment adjustments are made remotely using compact piezo-electric motors [15].

Diagnostics

Steering and alignment diagnostics are provided by 4 miniature CCD profile monitors located behind transport line and IP bench mirrors. They view the laser light directly through the partial transmission of the mirror. A frame grabber based video analysis system is used to monitor the position and size of the spot at each of the monitors.

At the monitor beyond the IP, where reliability and camera radiation damage are concerns, the 50μm spot generated by the re-imaging optics is transmitted by a 10,000 fiber fused silica bundle [16] from the high radiation area to a

monitor table. The coherent fiber bundle fluoresces and shifts the UV into visible. It has a diameter of 0.5mm and a single fiber diameter of 10μm. The IP assembly also has two fast diodes and a beam pickup electrode that are used for finding the relative timing of the laser and particle beams.

The transport line is protected from stray laser light using a CW He-Cad 350 nm λ alignment laser that is mode matched to the high power laser on the laser table. The 1mW He-Cad laser is ideal for this purpose since it's wavelength is very close to the tripled YLF wavelength. If the signal from the CW laser at the monitor beyond the IP is lost, the high power laser shutter will be closed in order to protect the transport from mis-steered high power laser pulses.

Laser

The laser system consists of a mode-locked 119MHz, 150ps pulse length, YLF oscillator seed laser and a YLF regenerative amplifier laser. Both lasers are lamp - pumped. The oscillator is locked to the 119MHz accelerator clock frequency with a acousto-optic amplitude modulator operating at the first sub-harmonic. A single 1nJ pulse from the oscillator is switched into the amplifier using two Pockels cells.

The amplifier has a gain of 10^6 in 20 passes and produces 10mJ pulses of 1047nm λ light at a repetition rate of 40Hz. After tripling, we observe 2mJ at 349nm .λ with the same pulse length. We chose YLF as the lasing material because of its reduced thermal lensing compared to YAG. After frequency tripling, a pinhole spatial filter is used to improve the beam shape. A small fraction of the light is diverted into a phase space monitoring diagnostic, consisting of a transport of roughly equal length to the main transport and a camera used for measuring beam size, before the entrance to the transport line. The laser beam quality, characterized by M^2, the deviation from diffraction limit, is measured to be M^2=1.1.

Performance

The number of detected gamma rays and degraded e+/e- is reduced about a factor of 20 from N_γ due to the finite acceptance of the detectors and transmission losses in the laser transport and IP system. Thus the expected signal at optimum overlap was about 800 degraded particles. The most difficult aspect of commissioning the monitor was establishing collisions for the first time. Laser timing and e+/e- beam x and y position must be adjusted in order to establish collisions. Since the e+/e- bunch length is short (σ_z~ 2mm), the overlap is dominated by the laser pulse length. The initial timing setup done with the pickup and fast diode was accurate to about 0.5ns. The search strategy we adopted was to scan perpendicular to the laser beam direction (up and down in fig. 2) with an un-focused e- beam (one with the waist at the e+/- IP, 29cm away). A signal of a few counts over background was visible for ±1mm along the laser path. Once collisions were first established, they could easily be re-established using the timing signals and the beam position monitors that surround the IP.

Scanning is done using controls similar to those used for the beam-beam deflection. With this system, the 120Hz beam is steered across the laser spot on a succession of pulses, with detector data recorded on each pulse. A typical background-subtracted scan is shown in figure 4. A scan like this one takes about 30 seconds to complete.

An accurate calibration procedure is required in order to get an estimate $\sigma_{x,y}$ from the measured σ_s. Unfortunately, it is not possible to directly measure, using an independent technique, the high power laser σ_0 in the IP. The technique chosen for obtaining an estimate of σ_0 involves operating the SLC at intensities 20% of nominal, performing all emittance and IP $\sigma_{x,y}$ optimization using the beam-beam deflection and comparing the results with σ_s. This test provided e+/- beams with a beam-beam deflection overlap $\sigma_{x,y}$ of 2.9 x 1.0μm (which, for equal e+/- $\sigma_{x,y}$, should give actual $\sigma_{x,y}$ of 2.1 x 0.7 μm). Laser profile measurements done at that time yielded 2.0 x 0.85μm σ_s. The results are consistent with a 0.4 to 0.5μm laser σ_0, 20% larger than design expectations but adequate for SLC use.

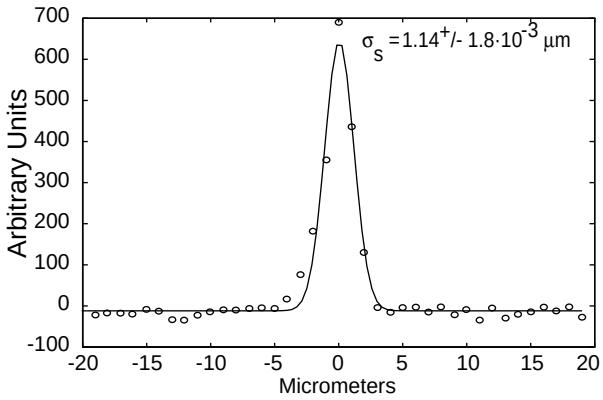

Figure 4. A typical profile monitor scan showing σ_{sy}. The horizontal scale is determined using the transfer matrix (R_{34}) for the scan coils to the laser IP. The collision signal in this case is detected using the SLD polarimeter degraded e- detector, located after the first large bend in the outgoing beamline. Each data point is the average of 3 beam pulses with the laser on, with the average of 6 pulses with the laser off subtracted.

Another measure of the system performance is a scan of the laser waist, shown in figure 5. In this scan, the e+/- beam is used to measure the divergence of the laser by making a series of σ_s measurements as it is steered along the laser path. In the waist scan, the effective divergence of the laser IP can be determined. The phase space volume of the laser beam cannot be determined from this scan since the contribution of the electrons to the minimum measured width is not accurately known.

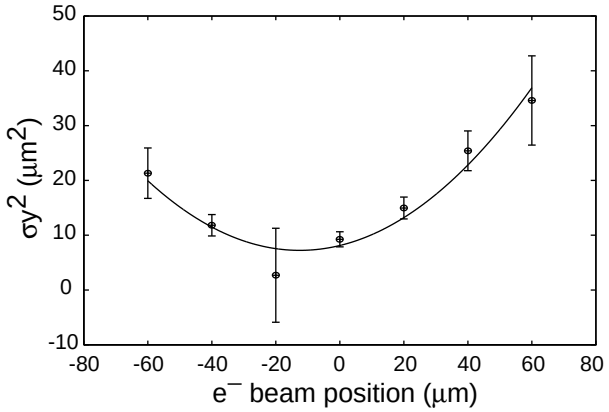

Figure 5. A typical laser-waist scan. The plot shows the measured σ_y^2 vs e- beam x position. A parabola is used for a fit.

Acknowledgments

We would like to acknowledge support for this project from the SLD collaboration, D. Burke and J. Sheppard. N. Phinney, P. Raimondi and F. Zimmermann helped with data acquisition and interpretation. Technical support from K. Ratcliffe, C. Rago, O. Millican, A. Farvid H. Baruz, K. Underwood and L. Hendrickson is also greatly appreciated. D. Meyerhofer of the University of Rochester gave much appreciated review and technical assistance during the course of the project.

References

[1] Emma, P., "The Stanford Linear Collider," Talk given at 16th IEEE Particle Accelerator Conference (PAC 95) and International Conference on High Energy Accelerators, Dallas, Texas, 1-5 May 1995.

[2] Koska, W., et.al., *Nucl.Instr.Meth.***A286**:32,1990.

[3] Shintake, T., et. al., "Design of Laser Compton Spot Size Monitor," Presented at 15th Int. Conf. on High-Energy Accelerators, Hamburg, Germany, Jul 20-24, 1992.

[4] Burke, D.L., "The Final Focus Test Beam Project," Presented at Particle Accelerator Conf., San Francisco, CA, May 6-9, 1991.

[5].Ross, M. C., et.al., "Wire Scanners for Beam Size and Emittance Measurements at the SLC," Presented at IEEE Particle Accelerator Conf., San Francisco, CA, May 6-9, 1991.

[6] Urakawa, J., Ed., "Sixth International Workshop on Linear Colliders, LC95", KEK 95-5, 1995.

[7] Siegman, A., '*Lasers*', University Science Books, 1986.

[8] Field, R. C., *Nucl.Instrum.Meth*. **A265**:167-169, (1988).

[9] Shapiro, G., et.al., "The Compton Polarimeter at the SLC," Presented at 1993 Particle Accelerator Conference (PAC 93), Washington, DC, 17-20 May 1993.

[10] SLD Collaboration (S. Hedges et al.).VXD3: The SLD Vertex Detector Upgrade Based on a 307 MPixel CCD System. Presented at the International Europhysics Conference on High Energy Physics Brussels, Belgium, 27 Jul - 2 Aug 1995.

[11] Bouwers, A., "*Achievements in Optics*", Elsevier, New York (1946). and Matsukov, D.D. *J. Opt. Soc. Am.*, **34**, pp. 270-284 (1944).

[12] Sharps, J., Package Induced Failure of Semiconductor Laser and Optical Telecommunication Components, Proceedings of SPIE **2714** 1995 p 676-677 and Guch, Steven Jr., et al. "Beyond perfection: the need for understanding contamination effects on real-world optics" Proceedings of SPIE **2114** 1994. p 505-511.

[13] Schermerhorn, Paul. Excimer laser damage testing of optical materials, Proceedings of SPIE - **1835** 1993. p 70-79.

[14] Cleveland Crystals, Cleveland, OH.

[15] New Focus Inc., Santa Clara, CA.

[16] Sumitomo Electric USA Inc., Los Angeles, CA.